



## A New Zealand White rabbit model of thrombocytopenia and coagulopathy following total body irradiation across the dose range to induce the hematopoietic-subsyndrome of acute radiation syndrome

Isabel L. Jackson , Ganga Gurung , Yannick Poirier , Mathangi Gopalakrishnan , Eric P. Cohen , Terez-Shea Donohue , Diana Newman & Zeljko Vujaskovic

To cite this article: Isabel L. Jackson , Ganga Gurung , Yannick Poirier , Mathangi Gopalakrishnan , Eric P. Cohen , Terez-Shea Donohue , Diana Newman & Zeljko Vujaskovic (2020): A New Zealand White rabbit model of thrombocytopenia and coagulopathy following total body irradiation across the dose range to induce the hematopoietic-subsyndrome of acute radiation syndrome, International Journal of Radiation Biology, DOI: [10.1080/09553002.2019.1668981](https://doi.org/10.1080/09553002.2019.1668981)

To link to this article: <https://doi.org/10.1080/09553002.2019.1668981>



Copyright © 2020 The Author(s). Published with license by Taylor & Francis Group, LLC.



View supplementary material [↗](#)



Published online: 05 Oct 2020.



Submit your article to this journal [↗](#)



Article views: 267



View related articles [↗](#)



View Crossmark data [↗](#)



Citing articles: 1 View citing articles [↗](#)

# A New Zealand White rabbit model of thrombocytopenia and coagulopathy following total body irradiation across the dose range to induce the hematopoietic-subsyndrome of acute radiation syndrome

Isabel L. Jackson<sup>a</sup>, Ganga Gurung<sup>a</sup>, Yannick Poirier<sup>a</sup>, Mathangi Gopalakrishnan<sup>b</sup>, Eric P. Cohen<sup>c</sup>, Terez-Shea Donohue<sup>a</sup>, Diana Newman<sup>a</sup>, and Zeljko Vujaskovic<sup>a</sup>

<sup>a</sup>Division of Translational Radiation Sciences, Department of Radiation Oncology, University of Maryland School of Medicine, Baltimore, MD, USA; <sup>b</sup>Center for Translational Medicine, University of Maryland School of Pharmacy, Baltimore, MD, USA; <sup>c</sup>Department of Medicine, University of Maryland School of Medicine, Baltimore, MD, USA

## ABSTRACT

**Purpose:** The purpose of this study was to develop a rabbit model of total body irradiation (TBI)-induced thrombocytopenia and coagulopathy across the dose-range which induces the hematopoietic subsyndrome of the acute radiation syndrome (H-ARS).

**Methods:** Twenty male New Zealand White rabbits were assigned to arms to receive 6-MV of TBI at a dose of 6.5, 7.5, 8.5 or 9.5 Gy. Animals were treated with moderate levels of supportive care including buprenorphine for pain management, antibiotics, antipyretics for rectal body temperature >104.8°F, and fluids for signs of dehydration. Animals were closely followed for up to 45 days after TBI for signs of major morbidity/mortality. Hematology and serum chemistry parameters were routinely monitored. Hemostasis parameters were analyzed prior to TBI, 2 and 6 hours post-TBI, and at the time of euthanasia.

**Results:** Animals developed the characteristic signs and symptoms of H-ARS during the first-week post TBI. Animals became thrombocytopenic with signs of severe acute anemia during the second week post TBI. Moribund animals presented with petechia and ecchymosis of the skin and generalized internal hemorrhage. Multiorgan dysfunction characterized by bone marrow failure, gastric ileus, acute renal toxicity, and liver abnormalities were common. Severe abnormalities in coagulation parameters were observed.

**Conclusions:** The presentation of bone marrow failure and multiorgan injury associated with ARS in the New Zealand White rabbit model is consistent with that described in the canine, swine, non-human primate, and in humans. The hemorrhagic syndrome associated with the ARS in rabbits is characterized by thrombocytopenia and hemostasis dysfunction, which appear to underlie the development of multiorgan dysfunction following TBI to rabbits. Taken together, the rabbit recapitulates the pathogenesis of ARS in humans, and may present an alternative small animal model for medical countermeasure pilot efficacy screening, dose-finding and schedule optimization studies prior to moving into large animal models of TBI-induced ARS.

## ARTICLE HISTORY

Received 27 June 2019  
Revised 9 September 2019  
Accepted 11 September 2019

## KEYWORDS



Total body irradiation; acute radiation syndrome; hematopoietic syndrome; coagulopathy; rabbit model


## Introduction

Acute radiation sickness (ARS) describes a constellation of syndromes that occur in the hours to weeks following whole body or significant partial body exposures to doses of 1 Gy or higher in humans (Hall and Giaccia 2011). The vast majority of our understanding regarding the biological effects of acute radiation exposure in humans comes from atomic bomb survivors from Hiroshima and Nagasaki (Liebow et al. 1949), accidentally exposed individuals on the Marshall Islands following experimental detonation of atomic bombs over the Bikini Atolls and accidents at nuclear installations (e.g. Chernobyl)(UNSCEAR 2000). In

humans, the signs and symptoms of ARS include fatigue, vomiting and diarrhea, myelosuppression and infections, petechial hemorrhages and ecchymosis, mucosal ulcerations, uncontrollable bleeding, and severe acute anemia (Warren 1946; Warren and Draeger 1946; Copley 1948; Liebow et al. 1949). Without medical intervention, the lethal dose for 50% of the population within the first sixty days (LD50/60) post-exposure is approximately 3.5 Gy (Hall and Giaccia 2011).

The temporal sequence of bone marrow aplasia associated with prompt radiation exposure to humans at doses  $\geq 2$  Gy follows a predictable course leading to complete hematological failure or spontaneous recovery. Lymphopenia is

**CONTACT** Isabel L. Jackson  [ijackson@som.umaryland.edu](mailto:ijackson@som.umaryland.edu)  Division of Translational Radiation Sciences, Department of Radiation Oncology, University of Maryland School of Medicine, 685 W. Baltimore Street, Medical Sciences Teaching Facility, Room 7-00A, Baltimore, MD 21201, USA

 Supplemental data for this article can be accessed [here](#).

Copyright © 2020 The Author(s). Published with license by Taylor & Francis Group, LLC.

This is an Open Access article distributed under the terms of the Creative Commons Attribution-NonCommercial-NoDerivatives License (<http://creativecommons.org/licenses/by-nc-nd/4.0/>), which permits non-commercial re-use, distribution, and reproduction in any medium, provided the original work is properly cited, and is not altered, transformed, or built upon in any way.

observed as early as the first day post-exposure. At the same time, a transient increase in granulocytes, termed an “abortive rise”, is observed prior to a steady decline that reaches a nadir around day 5. The observed rise is likely due to a mobilization of surviving progenitor cells and release of mature cells into the circulation and at supralethal exposures, may be absent altogether (Fliedner and Beyrer 2001). The early drop in the peripheral leukocyte count is followed by a progressive decline in platelet counts and development of a severe acute anemia during the second to third week post-exposure (Liebow et al. 1949). In the absence of spontaneous recovery associated with an increase in circulating leukocytes and platelets, death due to aplastic anemia, bacterial infections, and severe hemorrhage is common (Liebow et al. 1949). After the fourth week, multiorgan failure may occur, with stepwise development of injury to late responding normal tissues (e.g. pneumonitis, nephropathy) (Liebow et al. 1949).

In addition to the commonly described myelosuppression, petechiae and extensive ecchymosis in the skin, massive hemorrhages from body orifices along with prolonged bleeding times, are characteristic of a “severe hemorrhagic syndrome” and have been reported in victims with ARS (Warren 1946; Warren and Draeger 1946; Copley 1948). Following the atomic-bomb detonations over Hiroshima and Nagasaki, hemorrhagic deaths were observed between the third and fifth-week post-exposure concurrent with the period of severe thrombocytopenia (Warren 1946). Hemorrhagic lesions in the kidneys, stomach, gastrointestinal tract, and brain were observed at autopsy (Warren 1946).

Coagulopathy and hemorrhagic deaths in ARS mortality have not been fully elucidated. A number of limited studies have shown prolonged bleeding and clotting times, impaired clot retraction and extensive hemorrhage in large animals, similar to that also seen in humans (Cronkite 1950). Thrombocytopenia is typically cited as the cause of bleeding after radiation exposures, but this explanation may be incomplete. Elegant preclinical studies conducted by Allen and Jacobson in the canine found a bleeding diathesis following a dose of 4.5 Gy TBI that was associated with a heparin-like substance in the blood that prolonged clotting time when combined with blood from normal, unirradiated animals (Allen and Jacobson 1947). In those studies, anticoagulant activity was dissociated from thrombocytopenia and was reversed with anti-heparin agents both in vivo and in vitro (Allen and Jacobson 1947).

The objective of the current study was to define the temporal onset, progression, severity, and incidence profile of clinical signs and symptoms of hemostatic dysfunction and their relationship to major morbidity/mortality after graded single doses of TBI to induce bone marrow suppression associated with ARS in the male New Zealand White (NZW) rabbit. While the rodent is the most extensively used model to characterize ARS, the coagulation profile in rodents may not adequately translate to human. Therefore elucidating the role of coagulopathy in the context of TBI is limited when using a murine model (Siller-Matula et al.

2008). Rabbits, on the other hand, are the largest species within the small animal model category and present with a coagulation profile similar to humans. Therefore, the current study was designed to develop a rabbit model, as an alternative to the commonly used mouse or rat, to better examine and understand the pathogenesis of TBI-induced ARS in the context of hemostasis dysfunction with the eventual goal of medical countermeasures assessment. The rabbit presents an ideal alternative to the mouse or rat due to its larger size and therefore greater flexibility to serially assess the onset, severity, and progression of TBI-induced multiorgan injury through monitoring temporal changes in hematological parameters, biochemical markers of organ function, and hemostatic function.

## Materials and methods

### Animals

Twenty uncastrated male White New Zealand Rabbits (2.9–3.4 kg) were purchased from Charles River Laboratories, Wilmington, DE. Due to sex-differences in radiation dose-response in some species, only a single sex was chosen to minimize variability in the estimated lethality curves and reduce the sample size. Animals were singly housed and provided *ad libitum* access to reverse osmosis (RO) water by sipper lines connected to the building’s water supply. Animals were fed standard hay pelleted food and provided hay cubes and vegetables for enrichment. Housing facilities were maintained on a 12 h light/12 h dark cycle at 68–72 °F and 30–70% humidity. All procedures were performed in compliance with an animal use protocol approved by the University of Maryland, Baltimore Institutional Animal Use and Care Committee.

### Total body irradiation and methods to assure accuracy of dosing

The methodology for total body irradiation and dosimetry is described in Poirier et al. (Poirier et al. 2019). Briefly, a CT-based 3-dimensional “representative” dose calculation was performed on a single animal in advance of TBI in order to ensure the accuracy of irradiation (Poirier et al. 2019). Animals ( $n=5/\text{arm}$ ) were exposed to a single dose of 6.5 Gy, 7.5 Gy, 8.5 Gy, or 9.5 Gy TBI. Doses were selected based on re-analysis of the Pryor et al. (Pryor et al. 1967) dose-response in New Zealand white rabbits (LD50/30 ~ 9.7 Gy) with modification based on unpublished data. Briefly, animals were anesthetized by subcutaneous (SC) injection with ketamine (30–45 mg/kg)-xylazine (4.0–9.0 mg/kg) and placed at the location of the irradiation-unit’s isocenter for bilateral (left lateral and right lateral) irradiation. A 5 mm bolus was placed underneath the laterally recumbent animal to provide surface coverage to reduce the “skin sparing” entry dose profile of the beam and a beam spoiler consisting of acrylic plates was suspended a short distance above the animal to ensure the homogeneity of dose distribution (Poirier et al. 2019). TBI was delivered using parallel-

opposed 6 MV photons from a Varian True Beam clinical electron linear accelerator (LINAC). The target radiation dose was prescribed to the mid-depth plane at the level of the animal's mid-section. To ensure accuracy of radiation dose-delivery, optically stimulated luminescent dosimeters (OSLD) were placed (in pairs) on either lateral aspect of each animal, on the surface of the abdomen nearest to the animal's maximal width. Average measurements for individual animals absorbed dose were not more than 3.1% different from the targeted dose.

### **Cageside and clinical observations**

All animals were evaluated at least twice per day for changes in behavior, incidence, severity, and duration of soft stool or diarrhea, mobility/body position, and dehydration. All animals underwent a complete physical exam at least twice per week including rectal body temperature (RBT), heart rate/arterial blood oxygen saturation, respiratory rate, and body weight

### **Supportive care**

Animals were treated with enrofloxacin (Baytril, 2.5–5mg/kg, SC, QD) starting 24 h post TBI and continued daily until the study endpoint was reached (day 45). Tylenol (160 mg/mL) was administered to animals with RBT >104.8 °F. Buprenorphine (0.01–0.05 mg/kg, SC, BID) was administered on days 0 to 45.

### **Euthanasia and necropsy**

Animals meeting any one of the following criteria were euthanized to minimize pain and distress:  $\geq 20\%$  body weight loss, inability or extreme reluctance to stand persisting for 24 h, RBT <91.4 °C, severe acute anemia (<15% hematocrit or RBCs <3 × 10<sup>6</sup> cells/ $\mu$ L), or other signs of severe organ system dysfunction. For euthanasia, animals were sedated with ketamine (30–45 mg/kg, SC) -xylazine (4.0–9.0 mg/kg, SC) followed by administration of pentobarbital (>100mg/kg) intravenously followed by necropsy with tissue harvest after respiration ceased for >1 min. A gross evaluation of all vital organs was performed and documented at the time of necropsy. Tissue from the heart, lungs, spleen, liver, kidneys, mesenteric lymph nodes, thymus, small intestine, and colon, and blood samples were taken. Organ weights for the heart, lungs, kidney, and spleen were recorded.

### **Blood sampling for hematology, serum chemistry, whole blood thromboelastometry, and Routine-Laboratory coagulation/hemostasis tests**

Blood was sampled from the marginal ear vein at baseline and on study days 1, 3, 5, 7, 10, 14, 17, 20, 24, 27, 30, 45 post-TBI; and by cardiac puncture at scheduled or unscheduled euthanasia. The volume sampled was below the 14-day limit of 0.75% of the animal's body weight to avoid

hypovolemia and anemia. Serum chemistry and complete blood counts with five-part differentials were performed by Antech Diagnostics (Fountain Valley, CA 92708). for a lipid panel (e.g. cholesterol, triglycerides), renal function tests (e.g. blood urea nitrogen, calcium, chloride, creatinine, glucose, phosphorus, potassium, sodium), liver function tests [e.g. total protein, albumin, total bilirubin, alanine transaminase (ALT), aspartate transaminase (AST), alkaline phosphatase (ALP), gamma-glutamyl transpeptidase (GGTP), globulin, albumin/globulin ratio], and magnesium, chloride, amylase, and creatinine phosphokinase (CPK). Peripheral blood films were evaluated for cellular abnormalities by a board-certified veterinary pathologist. For routine-laboratory coagulation (e.g. hemostasis) tests, citrate-stabilized blood samples were drawn at baseline, at 2 - and 6 h post-TBI and at the time of scheduled or unscheduled euthanasia. Each animal served as its own control.

### **Thromboelastometry**

Viscoelastic hemostasis measurements were tested using Rotational Thromboelastometry (whole blood coagulation analyzer; ROTEM-Delta, TEM International) operated in native (NATEM) test mode. A correction formula for the adjustment of the citrate anticoagulant volume added to the collection tube was used to compensate for lower than normal hematocrit values.

### **Routine Laboratory-Based coagulation tests**

Routine coagulation tests were performed on a BCS XP fully-automated hemostasis analyzer (Siemens HealthCare, Newark, DE).

### **Thrombin generation assay**

Thrombin generation was measured using the Technothrombin<sup>®</sup> Thrombin Generation Assay (TGA; Technoclon GmbH, Vienna, Austria) performed according to the manufacturer's instructions. Quantitative measurement of thrombin generation was performed using the BIOTEK Synergy HTX multi-mode microplate reader (BioTek Instruments, Inc. Winooski, Vermont) and results analyzed using the BIOTEK FLx800 Gen5 software.

### **Enzyme-Linked immunosorbent assays (ELISA) for ADAMTS13, plasminogen and FDP**

Chromogenic ELISA for determination of ADAMTS13 activity was performed using the TECHNOZYME<sup>®</sup> ADAMTS13 Assay performed according to the manufacturer's instructions (Technoclon GmbH, Vienna, Austria). Plasminogen (ng/mL) was measured using the Rabbit Plasminogen ELISA Kit (Catalog Number: ab190544). Fibrinogen Degradation Products were determined using the rabbit Fibrinogen Degradation Product ELISA (LS-F22437, LifeSpan Biosciences). Negative controls were included with each assay for performance verification. All assays were

performed according to the manufacturer's instructions and plates read using the BIOTEK Synergy HTX multi-mode microplate reader (BioTek Instruments, Inc. Winooski, Vermont).

### Histopathology

Tissues were fixed in 10% neutral buffered formalin until processing for histology by the University of Maryland Pathology Associates (Baltimore, MD). Paraffin-embedded samples were sectioned at 5-micron-thickness and stained with Masson's Trichrome for analysis of architectural distortion, inflammation, and fibrosis.

### Data analysis

The probability of 45-day survival was estimated using the Kaplan-Meier method. The odds of TBI-induced mortality were determined by logistic regression analysis (p-value and 95% CI) on the occurrence of death and the lethal dose for 10–95% of animals within the first 45 days post-exposure estimated from the dose-mortality relationship. The probability of occurrence of thrombocytopenia (indicated by platelet counts) by dose was assessed by logistic regression analysis and Kaplan Meier curves for time to thrombocytopenia were obtained by radiation dose to assess median time to thrombocytopenia. The blood cell counts (lymphocytes, neutrophils, white blood cells) and different metrics of biomarkers such as change from baseline and % change from baseline were summarized using descriptive statistics (mean, standard deviation, median, maximum and minimum) at each time point by dose and extensive explorative graphical analysis was performed to examine the biomarker trends over time and was compared in animals that are survivors and decedents. All statistical analyses were performed as two-sided tests at  $\alpha = 0.05$ .

## Results

### 45-Day mortality

Twenty-percent of animals ( $n = 1/5$ ) exposed to 6.5 Gy TBI and 60% of animals ( $n = 3/5$ ) exposed to 7.5 Gy expired prior to the study endpoint of 45-days. There were no 45-day survivors among animals exposed to 8.5 ( $n = 0/5$ ) or 9.5 ( $n = 0/5$ ) Gy TBI (Figure 1(A)). All animals in this study expired between days 7 and 15 post-TBI. All animals in the 7.5 to 9.5 Gy TBI arms met the criteria for severe acute anemia (HCT <15%, RBC <  $3.0 \times 10^6/\mu\text{L}$ ) at the time of euthanasia. One animal (6.5 Gy) was euthanized for signs of severe organ dysfunction (e.g. lethargy and sunset eye phenomenon) attributed to febrile neutropenia (e.g. ANC = 6 cells/ $\mu\text{L}$  and RBT = 105.5 °F).

Logistic regression of Kaplan-Meier curves for 45-day survival (Figure 1(B)) estimate the lethal dose for 50% of animals within the first 45-days post-exposure (LD50/45) to be 7.19 Gy. Kaplan-Meier survival analysis did not demonstrate a significant correlation between animal respiratory

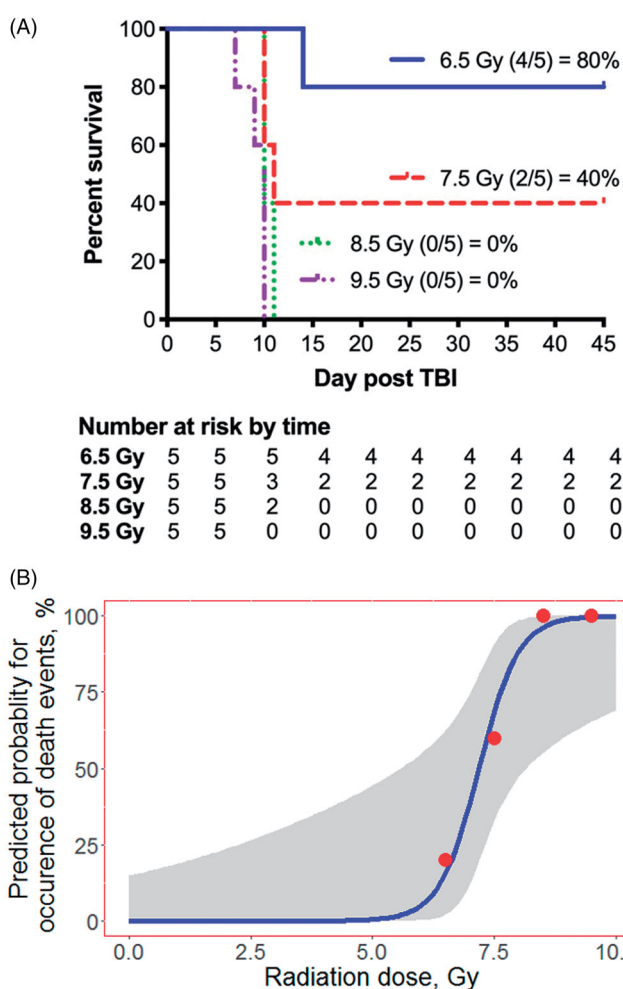


**Figure 1.** A. Kaplan-Meier curves for 45-day survival following exposure to 6.5 to 9.5 Gy of 6 MV photon total body irradiation (TBI). Animals were exposed to graded doses of total body irradiation (6.5 to 9.5 Gy, 1 Gy increments;  $n = 5/\text{dose}$ ). All animals succumbed to radiation-induced mortality between day 7 and day 15 postTBI. Animals surviving to day 15 demonstrated a recovery in hematological, serum chemistry, and clotting kinetics by day 45. On gross exam, no overt signs of tissue damage were noted. However, histology exam showed extensive pathology. B. Logistic-regression analysis for 45-day mortality with 95% confidence interval. The LD10 is estimated to be 6.30 Gy with 99% lethality at 9.05 Gy. The LD50 is estimated to be 7.19 Gy and the LD70 is estimated to be 7.53 Gy.

rate ( $p = .94$ ), SpO2 ( $p = .32$ ), heart rate ( $p = .48$ ), or rectal body temperature ( $p = .19$ ) and mortality.

### Hematological changes associated with acute, total body irradiation in the NZW rabbit

Results of repeat hematological analysis demonstrated a progressive decline in white blood cell (WBC) counts over the course of the first five days post-exposure (Figure 2(A)). The WBC nadir was radiation dose-dependent with the lowest counts observed on approximately the 5<sup>th</sup> day post-TBI in the 8.5 and 9.5 Gy arms. Lymphocytes were depleted as early as the first-day post-exposure (Figure 2(B)). At this time, neutrophil mobilization was evident and was followed by a rapid decline through day 3 post-TBI (Figure 2(C)). This was followed by a transient

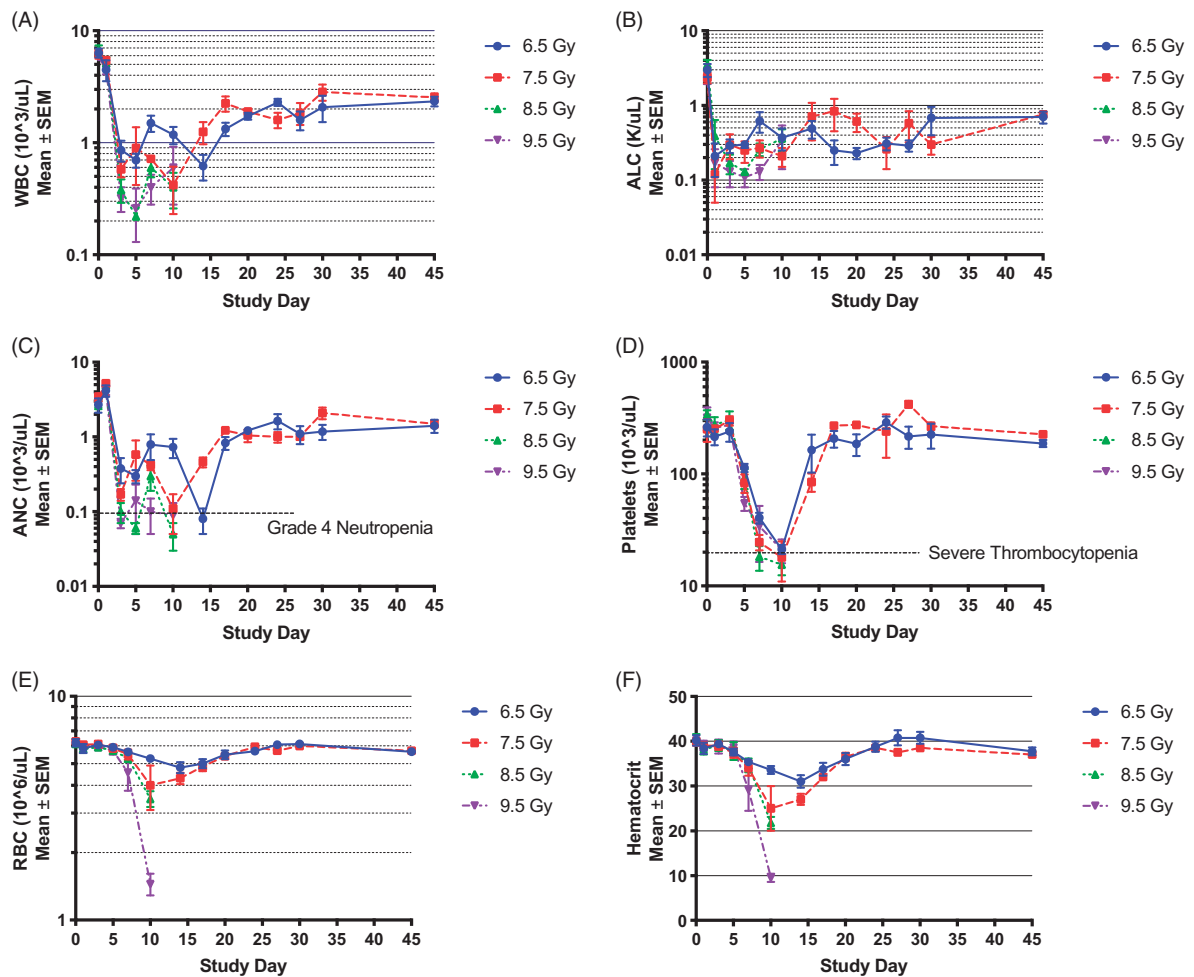


**Figure 2.** Bone marrow failure following TBI in the NZW rabbit presented by radiation dose. Complete blood count with differential was performed by Antech Diagnostics, Inc., on samples collected at baseline (-5 day), and at day 1, 3, 5, 7, 10, 14, 17, 20, 27, 30, and 45 post-TBI. The familiar drop in white blood count (WBC) count (A), absolute lymphocyte cell (ALC) count (B) and absolute neutrophil count (ANC, C) is evident, suggesting the model presents with bone marrow failure as expected following total body irradiation (TBI) across the dose range between 6.5 to 9.5 Gy. Platelets (D) red blood cell (RBC) counts (E), and hematocrit (F) began to decline on the fifth to seventh day post-exposure and reached a nadir during the second week post-TBI. Data in panels A-E are presented on a log-scale as mean  $\pm$  SEM. Data in panel 5 is presented on a linear scale as mean  $\pm$  SEM.

**Table 1.** Neutrophil related parameters in New Zealand rabbits after total body irradiation.

Radiation arm (n)		Time (days) to First day ANC		Time (days) to Last day ANC		Duration (days) of ANC		Recovery (days) to ANC $\geq$ 1000 cells/uL	ANC Nadir $\times$ 1000 cells/uL
		<500 cells/uL	<100 cells/uL	<500 cells/uL	<100 cells/uL	<500 cells/uL	<100 cells/uL		
6.5 Gy (n=5)	Mean $\pm$ SD	5.2 $\pm$ 4.9	14 <sup>a</sup>	17.8 $\pm$ 1.5	15.3 $\pm$ 3.5	12.0 $\pm$ 6.2	3 <sup>a</sup>	18.5 $\pm$ 1.7	54.4 $\pm$ 41.7
	Median	3	14	17	17	14	3	18.5	63
	Range	(3, 14)	NA	(17, 20)	(10, 17)	(3, 7)	NA	(17, 20)	(6, 105)
7.5 Gy (n=5)	Mean $\pm$ SD	3 <sup>a</sup>	8.3 $\pm$ 3.5	15.5 $\pm$ 2.1	7.3 $\pm$ 5.9	12.5 $\pm$ 2.1	3 $\pm$ 1.4	17	45.0 $\pm$ 53.3
	Median	3	10	15.5	5	12.5	3	17	14
	Range	NA	(3, 10)	(14, 17)	(3, 14)	(11, 14)	(2, 4)	NA	(3, 114)
8.5 Gy (n=5)	Mean $\pm$ SD	3 <sup>a</sup>	3.8 $\pm$ 1.1	NA <sup>b</sup>	6.0 $\pm$ 1.4	NA	3 $\pm$ 1.4	NA	19.2 $\pm$ 21.1
	Median	3	3	NA	6	NA	3	NA	15
	Range	NA	(3, 5)	NA	(5, 7)	NA	(2, 4)	NA	(0, 48)
9.5 Gy (n=5)	Mean $\pm$ SD	3 <sup>a</sup>	4.4 $\pm$ 3.1	NA	10	NA	NA	NA	12.6 $\pm$ 16.5
	Median	3	3	NA	10	NA	NA	NA	2
	Range	NA	(3, 10)	NA	NA	NA	NA	NA	(0, 36)

The time to first day and last, where the absolute neutrophil counts are less than < 500 cells/uL (e.g. neutropenia) and 100 cells/uL (e.g. severe neutropenia) are reported. The duration of neutropenia was estimated as the number of days that an animal had an observed ANC below 500 cells/uL or 100 cells/uL. The nadir was the lowest observed ANC in cells/uL during the 45-day trial. Data only include values obtained from peripheral blood samples at scheduled timepoints.

<sup>a</sup>SD not reported since the values were the same for all the animals; <sup>b</sup>Could not be calculated because the value was the same for all animals or could not be calculated.

rise in absolute neutrophil count prior to a second wave of decline between days 10 and 15 (Table 1). Features of infection and sepsis, such as toxic granulation and left shift of neutrophils on peripheral blood smears were infrequent or absent, respectively.

### Correlation of thrombocytopenia, hemorrhage, and anemia with major morbidity/mortality

Platelet counts of  $<75,000$  cells/ $\mu\text{L}$  (Figure 2(D)) and severe acute anemia (hemoglobin  $<6.8$  g/dL, RBC  $<3.2 \times 10^6/\mu\text{L}$ , Figure 2(E)) were significantly associated with mortality ( $p = .0027$  and  $p = .00098$ , respectively). The temporal onset

**Table 2.** Platelet related parameters in New Zealand rabbits after total body irradiation.

Radiation arm (n)		Time (days) to First day Platelet count $<50,000$ cells/uL or $<20,000$ cells/uL		Time (days) to Last day Platelet count $<50,000$ cells/uL or $<20,000$ cells/uL		Duration (days) of Platelet count $<50,000$ cells/uL or $<20,000$ cells/uL		Recovery (days) to Platelet count $>50 \times 10^3$ cells/uL	Platelet Nadir $\times 1000$ cells/uL
		$<50 \times 10^3$ cells/uL	$<20 \times 10^3$ cells/uL	$<50 \times 10^3$ cells/uL	$<20 \times 10^3$ cells/uL	$<50 \times 10^3$ cells/uL	$<20 \times 10^3$ cells/uL		
6.5 Gy (n = 5)	Mean $\pm$ SD	$7.6 \pm 1.3$	$10.0^a$	$15.2 \pm 1.6$	$12.4 \pm 2.2$	$7.6 \pm 2.5$	4	$15.2 \pm 1.6$	$21.2 \pm 4.4$
	Median	7	10	14	14	7	4	14	20
	Range	(7, 10)	NA	(14, 17)	(10, 14)	(4, 10)	NA	(14, 17)	(17, 28)
7.5 Gy (n = 5)	Mean $\pm$ SD	$6.6 \pm 0.9$	$8.5 \pm 1.7$	14	$10.5 \pm 4.9$	7.0	7	14	$13.8 \pm 10.5$
	Median	7	8.5	14	10.5	7	7	14	14
	Range	(5, 7)	(7, 10)	NA <sup>b</sup>	(7, 14)	NA <sup>b</sup>	NA <sup>b</sup>	NA <sup>b</sup>	(4, 29)
8.5 Gy (n = 5)	Mean $\pm$ SD	$6.6 \pm 0.9$	7	NA	10	NA	3	NA	$14.4 \pm 6.1$
	Median	7	7	NA	10	NA	3	NA	16
	Range	(5, 7)	NA <sup>b</sup>	NA	NA	NA	NA	NA	(7, 21)
9.5 Gy (n = 5)	Mean $\pm$ SD	$6.2 \pm 1.1$	$7.8 \pm 1.5$	NA	$8.5 \pm 2.1$	NA	0	NA	$12.6 \pm 7.3$
	Median	7	7	NA	8.5	NA	0	NA	11
	Range	(5, 7)	(7, 10)	NA	(7, 10)	NA	NA	NA	(4, 22)

<sup>a</sup>SD not reported since the values were the same for all the animals; <sup>b</sup>Could not be calculated because the value was the same for all animals or could not be calculated. Data only include values obtained from peripheral blood samples at scheduled timepoints. Thrombocytopenia: Platelet count  $<50,000$  cells/uL; Severe thrombocytopenia: Platelet count  $<20,000$  cells/uL.

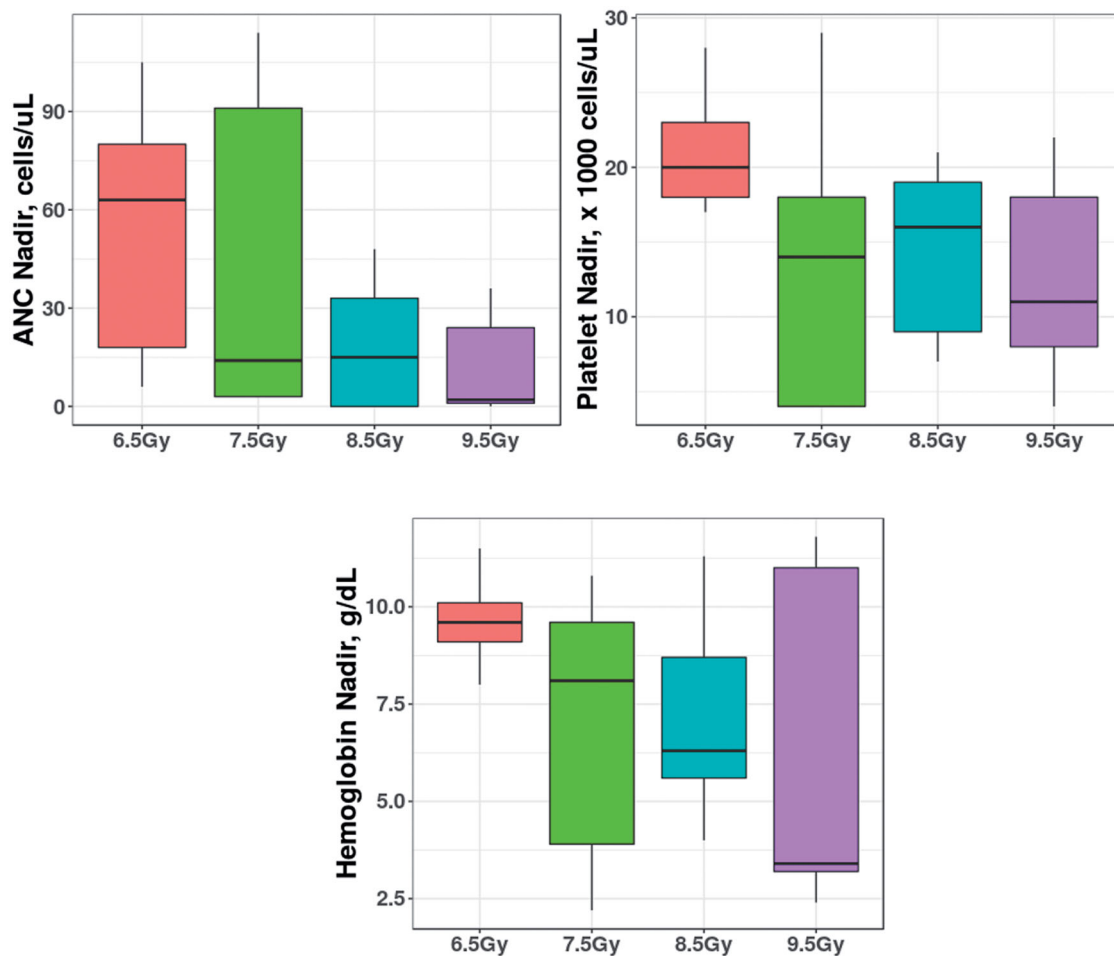


**Figure 3.** Boxplots of nadirs of ANC, Platelets and Hemoglobin in New Zealand Rabbits. The differences in the absolute nadir value between different radiation arms were not significantly different.

and duration of thrombocytopenia was radiation dose – dependent. Full recovery was observed 14–15 days post-onset at 6.5 to 7.5 Gy TBI (Table 2). At the highest radiation doses of 8.5 to 9.5 Gy, animals expired prior to recovery. There were no significant radiation dose-dependent differences in the nadirs for ANC, platelet counts, or hemoglobin (Figure 3).

Moribund animals generally presented with consistent decreases in packed cell volume (PCV determined by micro-hematocrit), severe thrombocytopenia (platelet count <20,000 cells) with absence of a regenerative (bone marrow) response, generalized petechiae and ecchymosis of the skin, severe hemorrhagic anemia, and gross hemorrhage of vital organs (e.g. stomach, small and large intestine, kidneys, Figure 4) at necropsy. Moribund animals often presented with pale ears and animals were cold to the touch. Prolonged activated partial thromboplastin time (aPTT), elevated fibrinogen levels, and/or increased antithrombin activity were common features in animals euthanized prior to the study endpoint of 45-days.

One animal in the 6.5 Gy TBI arm was euthanized due to fever (>105 °F), tilted head, and “setting sun” eye phenomena indicative of increased intracranial pressure (Cernerud 1975), but did not exhibit signs of hemorrhage observed in moribund animals at doses of 7.5 Gy or higher. At the time of euthanasia, the animal presented with normal platelet counts, red blood cell count and hematocrit; but was severely neutropenic (ANC <500 cells/ $\mu$ L) with a 2-fold increase in fibrinogen and elevated antithrombin activity.

Four of the five surviving animals presented with nucleated red blood cells between days 7 and 20-post-TBI, which was supportive of a regenerative response by the bone marrow. Only one decedent (e.g. euthanized prior to the 45-day study endpoint) presented with very rare nucleated red

blood cells (e.g. 1 per 100 cells). This was observed on day 1 post-TBI and was considered an unreliable finding unlikely to be of significance. Polychromatophilic erythrocytes, a sign of bone marrow stress, were noted on peripheral blood smears between days 1 and 10, but did not appear to be correlated with outcomes. Fibrin clots were observed on the blood films between days 3–7 post TBI in seven of twenty-animals, which was not associated with survival outcomes. These features did not appear to correlate with outcomes. Features of microangiopathic hemolytic anemia (e.g. schistocytes) were notably absent.

#### **Hemostasis dysfunction (coagulopathies) associated with ARS**

Blood was sampled at the time of unscheduled or scheduled euthanasia and stabilized in 3.8% sodium citrate for analysis of plasma-based biomarkers associated with hemostasis dysfunction. Viscoelastic hemostatic assays (e.g. rotational thromboelastometry) showed severe hemostatic dysfunction at the time of imminent mortality. For the NATEM test, clotting time (CT, Figure 5(A)) and clot formation time (CFT, Figure 5(B)) were markedly prolonged in comparison to baseline measurements at doses of 7.5 Gy and higher. This was associated with decreased maximum clot firmness (MCF; Figure 5(C)) suggesting weak clot formation. Alpha ( $\alpha$ )-angles (Figure 5(D)) were significantly lower at the time of morbidity. One limitation to the study is the analysis of rotational thromboelastometry at the time of unscheduled or scheduled euthanasia, which prohibited comparison of clotting kinetics/function with 45-day survivors at the same time point.

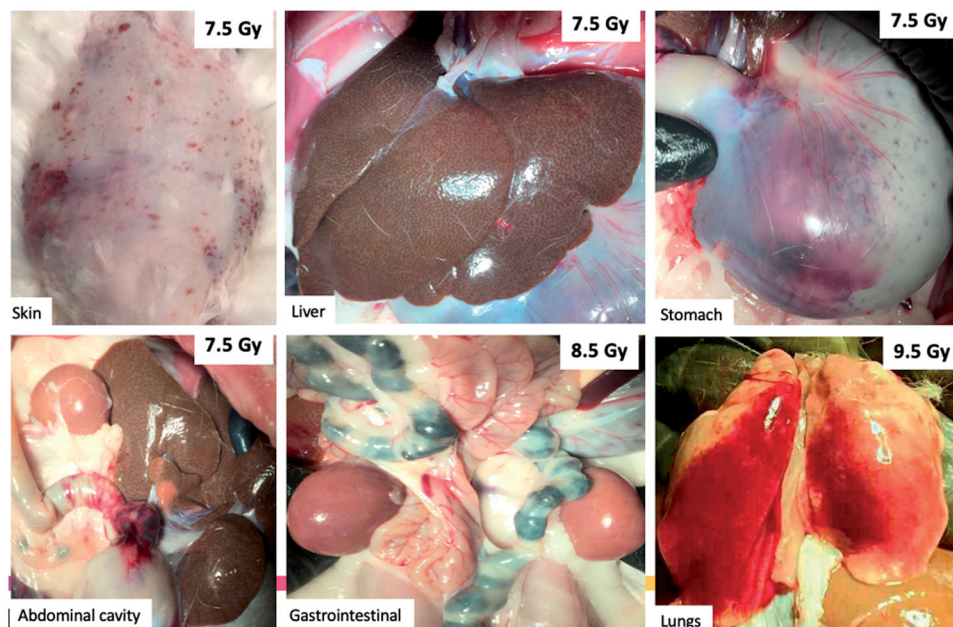


**Figure 4.** Gross hemorrhage observed in the skin and vital organs at necropsy. Representative photographs of gross abnormalities in vital organs were taken at necropsy. Moribund animals presented with visible petechial hemorrhage in the skin, mottled liver, bleeding in the stomach, abdominal cavity, and gastrointestinal tract at TBI doses of 7.5 Gy and higher. Hemorrhage was also observed in the lungs, but it was unclear whether this was due to cardiac puncture at the time of euthanasia or due to TBI.



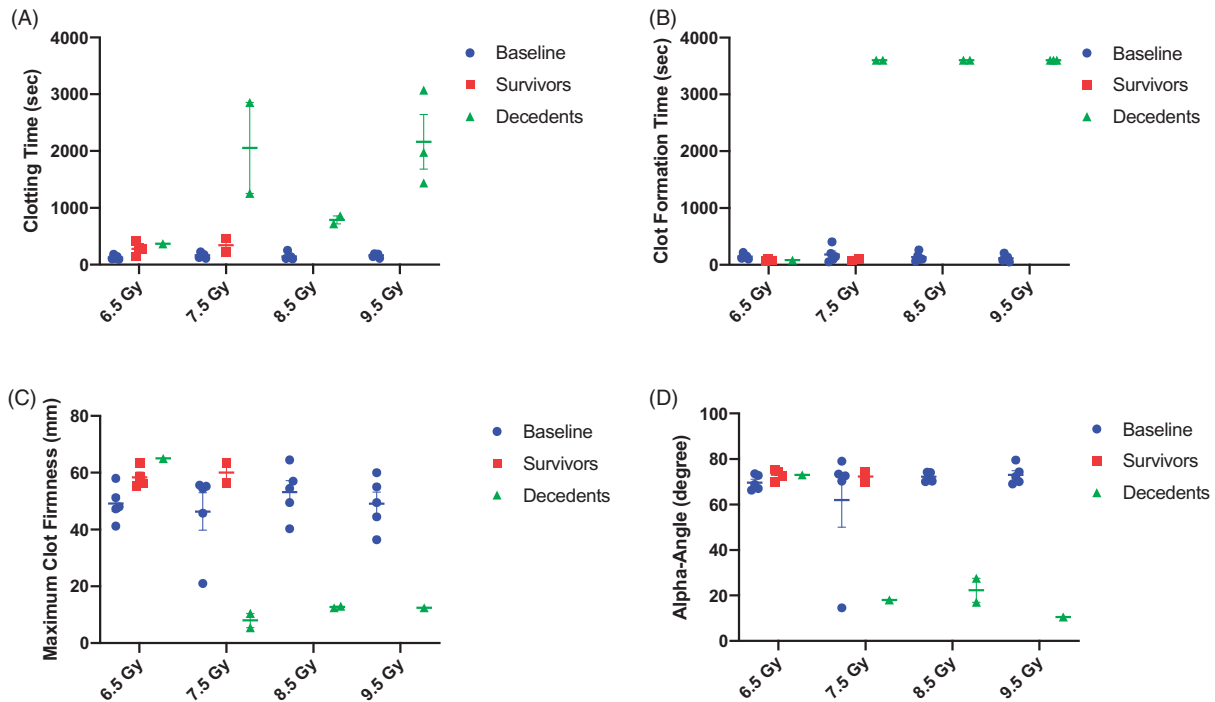


**Figure 5.** Evaluation of clotting parameters using rotational thromboelastometry (ROTEM) performed on whole blood at baseline and at the time of scheduled or unscheduled euthanasia. (A) Among animals expiring prior to the 45-day study endpoint (e.g. decedents), clotting time was severely prolonged in comparison to baseline draws. Clotting times among 45-day survivors at 6.5 and 7.5 Gy was slightly longer compared to baseline but did not reach statistical significance (paired t-test,  $p > .05$ ). (B) No significance differences were observed in clot formation time between 45-day survivors and baseline values. In contrast, blood drawn from decedents at 7.5 to 9.5 Gy was unable to clot. In this graph, 3600 s was used to represent a 60 min run without clot formation. (C) 45-day survivors showed a trend towards increased maximum clot firmness suggesting stronger clot formation at the scheduled study endpoint compared to baseline, although this did not reach significance ( $p > .05$ ). In contrast, maximum clot firmness among decedents, when evaluable, was severely reduced. Maximum clot firmness was not reported in all decedents due to platelet deficiency. (D) The alpha-angle was similar among all subjects at baseline except for one outlier in the 7.5 Gy TBI cohort. The outlier in the 7.5 Gy arm was consistently lower than for all other animals over three blood draws on separate days. 45-day survivors presented with a similar alpha-angle as the baseline values. In decedents at 7.5 to 9.5 Gy, a decrease in the alpha angle was noted.

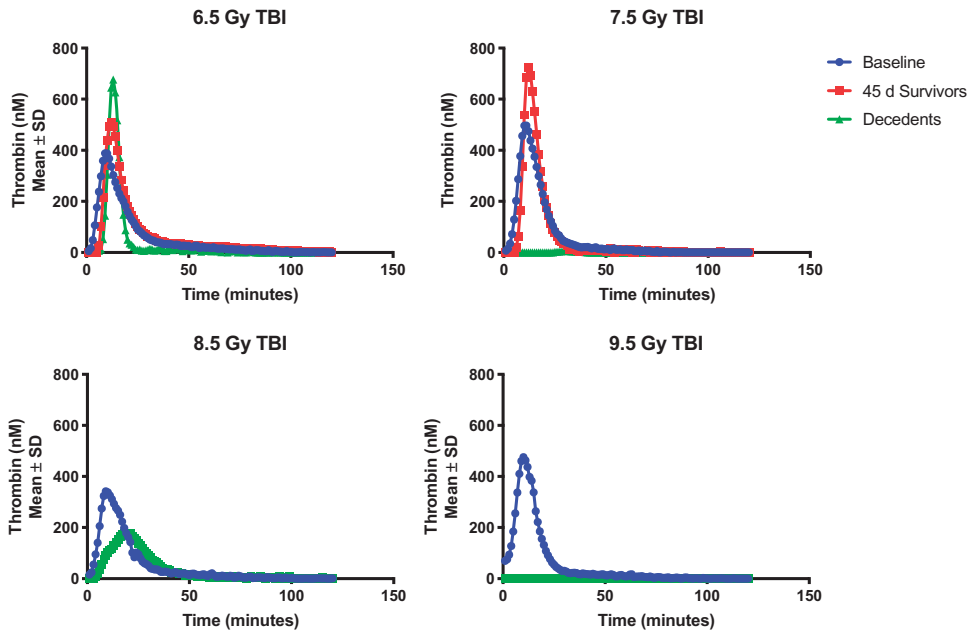


**Figure 6.** Inhibition of thrombin generation at time of scheduled or unscheduled necropsy is observed in animals euthanized prior to the 45-day study endpoint. Thrombin generation was severely inhibited among animals euthanized prior to the study endpoint due to meeting the criteria for imminent mortality. Data is reported as the peak height (Thrombin, nM), lag time, time to peak, and estimated potential for thrombin generation (area under the curve).

Data suggest a hypocoagulable state at the time of euthanasia due to criteria at TBI doses of 7.5 Gy and higher. Thrombin generation was notably reduced, or in some cases,

absent at the time of unscheduled euthanasia (Figure 6). At 6.5 and 7.5 Gy TBI, there appeared to be an increase in thrombin generation among survivors, suggesting a pro-

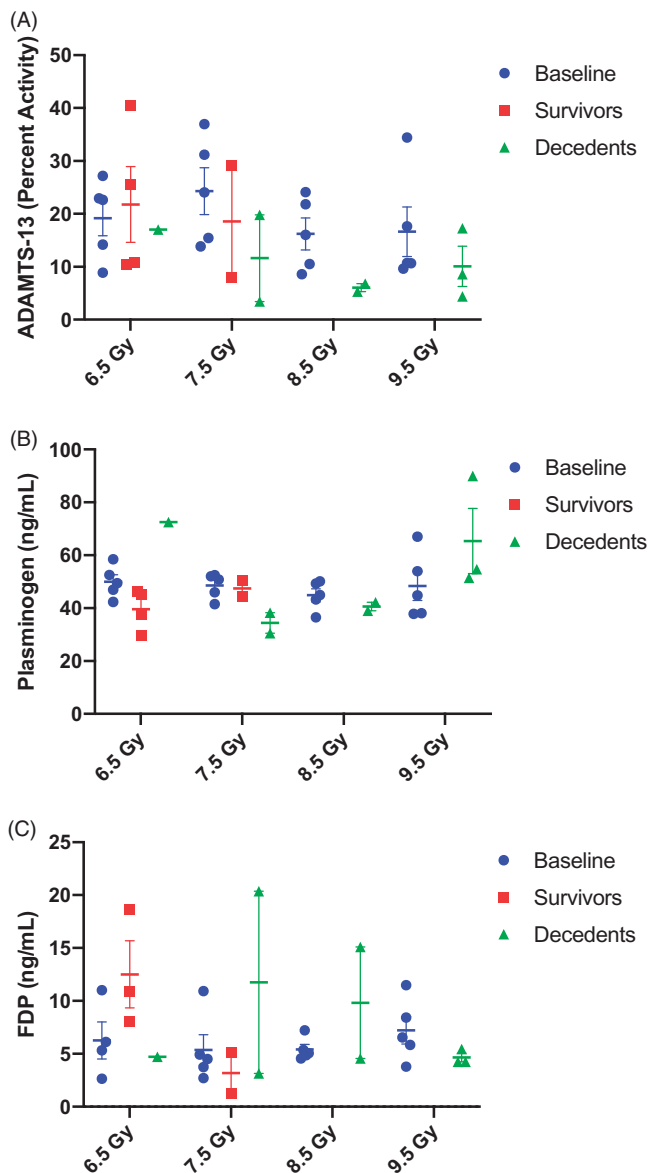


**Figure 7.** ADAMTS13 percent activity, plasminogen, and fibrin degradation products.

thrombotic state 45-days post exposure. There also appeared to be a radiation-dose dependent decrease in ADAMTS13 activity (Figure 7(A)), reminiscent of thrombotic thrombocytopenic purpura (TTP) in decedents. There did not appear to be associations between plasminogen levels and TBI dose or outcome (Figure 7(B)). The level of fibrin degradation products (FDP, Figure 7(C)) was variable across radiation-doses. FDP appeared to be elevated among 45-day survivors exposed to a TBI dose of 6.5 Gy; whereas FDP was decreased relative to baseline among decedents in the 7.5 and 8 Gy arms.

### **Serum chemistry markers of organ dysfunction and failure**

In this study, calcium levels were generally decreased in moribund animals and blood urea nitrogen (BUN) was

increased (data not shown). Creatinine at the time of euthanasia was above normal physiological limits in animals exposed to 9.5 Gy compared to 6.5 Gy. However, not all animals presented with elevated creatinine and BUN at the time of unscheduled euthanasia. There were no changes in bilirubin, suggesting that microangiopathic hemolytic anemia was not a cause of death among these animals. Total protein and albumin concentrations were low in all animals at the time of euthanasia, regardless of the time point. There was a dose-response increase in glucose concentration at the time of necropsy, but levels generally remained within the normal range.

### **Histopathologic damage associated with multiorgan injury and failure following TBI**

Across all radiation doses, there was more damage to the small intestine than the colon. There were no significant differences in the radiation-induced effects on morphology along the duodenum, jejunum, and ileum. Six animals in the 6.5 Gy (4/5) and 7.5 Gy (2/5) arms survived to day 45 and these survivors exhibited significant dose-dependent damage to the small intestine (Figure 8(A)). Microscopic exam revealed dilation of submucosal blood vessels, elongation of crypts, loss of surface epithelial cells, and mucosal hemorrhage. Among animals expiring prior to the study endpoint, damage to the small intestine was variable. Intact villi, with loss of epithelial cells particularly at tips were observed along the length of the small intestine. There was a slightly greater radiation-induced effect on the distal versus the proximal colon with evidence of abnormal crypts and increased mucosal depth (Figure 8(B)).

### **Discussion**

The objective of the current study was to establish an institutional lethality profile for 45-day mortality and characterize the natural history of the acute radiation syndrome (ARS) in the New Zealand White (NZW) rabbit model following total body irradiation (TBI) across the dose-range to induce bone marrow failure. The rabbit model was selected for these studies based on the general acceptance of this species as an alternative to the more commonly used rodent models (e.g. mice, rats) for therapeutic studies in small animal models to support product approval through the U.S. Food and Drug Administration (FDA). The rabbit model is presented as an alternative to the mouse-model for new target identification and medical countermeasure (MCM) efficacy screening in anticipation of product development and approval under the FDA animal rule (AR) regulatory pathway. The AR requires demonstrated efficacy in two species expected to react with a response predictive for humans acutely exposed to suprathreshold doses of ionizing radiation. Furthermore, the animal study endpoints must be clearly related to the desired benefit in humans and phylogenetically the rabbit may be closer to the human in expected responses (Mapara et al. 2012). In addition, the rabbit is the largest species within the small animal category

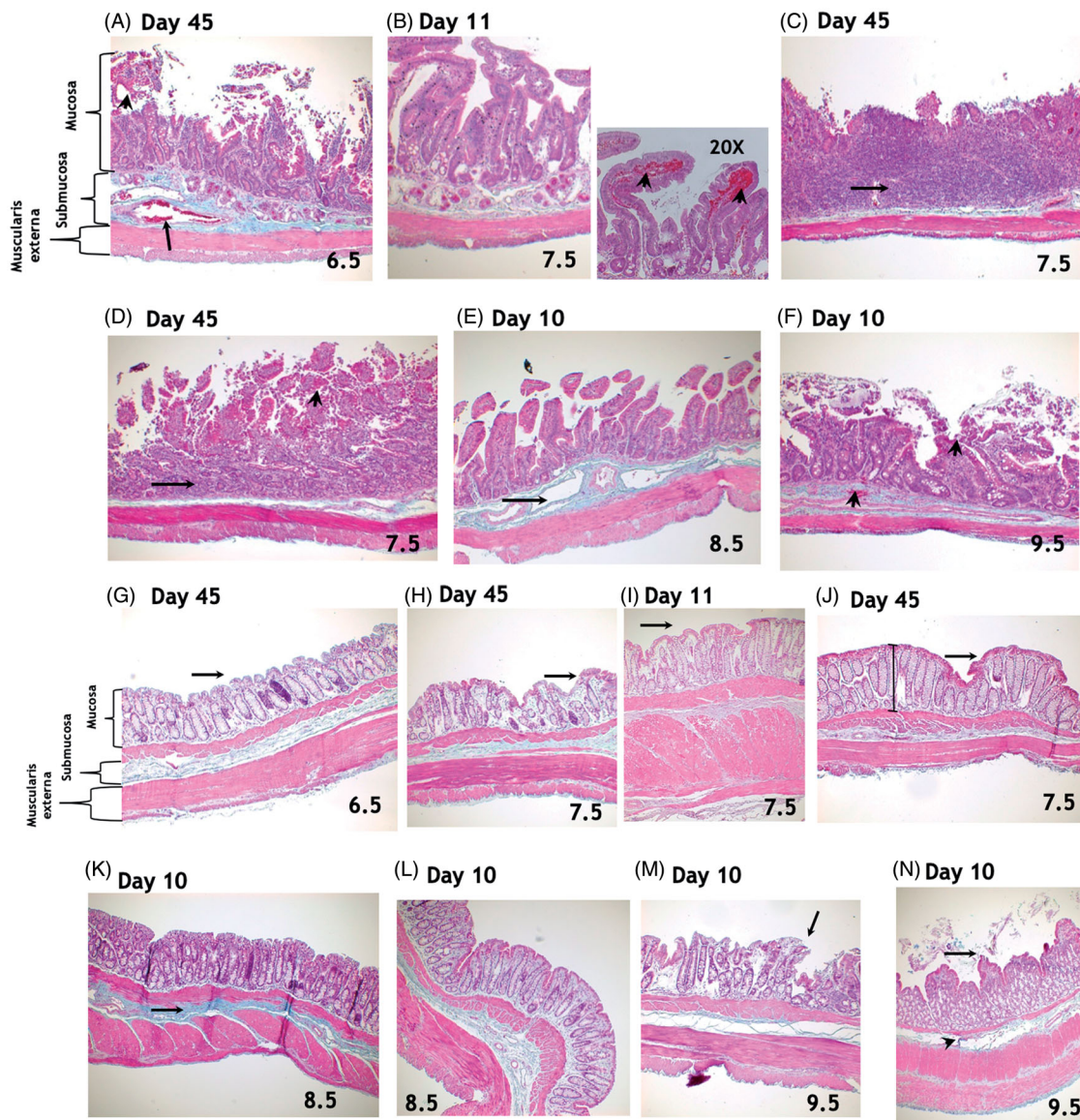


**Figure 8.** Top Panel: Masson's trichrome staining of the small intestine. There were no significant differences in radiation-induced effects in the duodenum, jejunum, or ileum. (A) Microscopic exam of small intestines from animals exposed to 6.5 Gy TBI and surviving to day 45 reveals dilation of submucosal blood vessels (arrow), elongation of crypts, loss of surface epithelial cells, and mucosal hemorrhage (arrow head). (B) Findings in animals exposed to 7.5 Gy and euthanized during the second week included intact villi but with loss of epithelial cells, particularly at the tips along the length of the small intestine. Mucosal hemorrhage (arrowheads in 20X photomicrograph) was also a histological feature at this time. (C–D) At 45-days post-exposure to 7.5 Gy TBI, complete loss of villi and crypts with replacement by inflammatory infiltrate (arrows) and mucosal hemorrhage (arrowhead) were observed, suggesting persistent GI damage. (E) Damage to the small intestine was variable among animals in the 8.5 to 9.5 Gy arms that expired prior to the study endpoint of 45-days. Findings include evidence of submucosal edema and vasodilation (arrow, E). (F) Epithelial sloughing, loss of villi and crypts, mucosal and submucosal hemorrhage (arrowheads) were observed. All images were taken at 10X magnification, unless otherwise noted above. Bottom Panel: Masson's trichrome staining of the colon. Overall, there was less damage to the colon than to the small intestines at all radiation doses. Animals exposed to 6.5 or 7.5 Gy TBI and surviving to day 45 had mostly intact epithelial layers in the colon (arrows, G–J). Findings included abnormal crypts (I, J) and increased mucosal depth (shown by lines in J). In animals exposed to 8.5 and 9.5 Gy, damage to the colon was somewhat variable. Findings included increased deposition of collagen strands in the submucosa (K, arrow), loss of surface epithelial cells (arrows, L, M) and disorganized crypts (L – N). All images were taken at 10X magnification, unless otherwise noted above.

with sufficient blood volume for repetitive sampling. Serial monitoring of dynamic changes in biomarkers associated with the onset, severity, and progression of multiorgan injury improves the capability to compare and contrast the individual species response with the expected human reaction to TBI.

In the NZW rabbit model of ARS, the extent of morbidity/mortality was inversely proportional to the absorbed TBI dose (Figure 1(A)). Animals exposed to doses in the range of 7.5 to 9.5 Gy TBI met the criteria for imminent mortality

primarily during the second week post-TBI. Logistic-regression of 45-day Kaplan-Meier survival generated in this study shows the LD50/45 in the NZW rabbit model to be 7.19 Gy (Figure 1(B)). It is important to remember the sensitivity to radiation varies both within and across species. For example, in humans, the lethal dose for 50% of the population within 60 days (LD50/60) of the exposure is approximately 3.5 Gy in the absence of therapeutic intervention. With supportive care including fluids, antibiotics, cytokine therapy, and transfusions, the LD50/60 can be increased to approximately

5.5 Gy. In contrast, the LD50/60 in the non-human primate is estimated between 6.5 to 7.8 Gy with intensive medical intervention. The LD50/60 is significantly lower in the minipigs and canine and is approximately 1.8–2.5 Gy (Moroni et al. 2011) and 2.5 to 3.5 Gy (Norris et al. 1968; Norris and Poole 1968), respectively. Regardless of the LD50/60, the pathology of ARS is similar across the minipig, canine, and non-human primate, and bears a striking resemblance to that observed in humans.

In this study, major morbidity in the NZW rabbit was primarily characterized by bone marrow failure (Figure 2(A–F)) with Grade 3–4 neutropenia ( $<1000$  cells/ $\mu\text{L}$ ) (Figure 2(C)), Grade 3 thrombocytopenia ( $<20,000$  cells/ $\mu\text{L}$ , Figure 2(D)), and severe abnormalities in whole blood viscoelastic parameters. The precipitous drop in hematocrit over a period of days to hours (Figure 2(F)) was associated with severe, uncontrolled bleeding characterized by petechiae, ecchymosis, and internal hemorrhage (Figure 4). The presence of a severe hemorrhagic syndrome associated with bone marrow failure are consistent with that described in other animal species (Allen and Jacobson 1947; Cronkite 1950) and humans exposed to prompt doses of ionizing radiation (Liebow et al. 1949).

The fall in hematocrit and red blood cell counts was an ominous sign for impending mortality. In moribund animals, the hematocrit fell 50% or more over a two to three-day period prior to animals meeting the criteria for unscheduled euthanasia. Thrombocytopenia always preceded the onset of severe anemia. The rapid decline in hematocrit coincident to the presentation of hemorrhage and absence of schistocytes on the peripheral blood films suggest that hemolytic anemia was not the cause of death among these animals. Infection and septicemia were also unlikely to be a major cause of morbidity/mortality; however, the administration of antibiotics to study animals may have reduced the propensity for infection.

Consistent with gross findings, architectural damage and inflammation evident upon histological exam suggests this is a multiorgan injury model (Figure 8). Gross exam at the time of necropsy revealed paralytic ileus in all of animals, which is a well-known gastrointestinal complication associated with radiation. Paralytic ileus is recognizable by diminished or absent bowel sounds upon clinical exam, diminished bowel production, and grossly distended stomach and intestines upon necropsy. Microscopic exam of the small and large intestine showed pathologic features consistent with the gastrointestinal-subsyndrome of ARS. Across all radiation doses, there was more damage to the small intestine than the colon, which is consistent with that previously observed in the non-human primate (MacVittie et al. 2012; Shea-Donohue et al. 2016). While the increase in blood urea nitrogen levels at the time of unscheduled euthanasia was suggestive of acute renal failure, microscopic exam showed only scattered tubular injury in animals exposed to doses of 7.5 Gy or higher. Occasionally, tubules showed cellular disorganization (e.g. 1 in 10). However, the glomeruli and blood vessels were normal.

Data generated in this study indicate a radiation-dose dependent increase in bone marrow failure and a reduction in thrombin, fibrinogen, and platelet activity. Data also demonstrate a dose-dependent reduction in ADAMTS 13 activity (Figure 7), as well as elevated fibrinogen and increased antithrombin activity among some animals that were euthanized due to criteria. Amongst animals exposed to 7.5 to 9.5 Gy TBI, mortality was predominantly hemorrhage or rapid demise of unknown etiology. Sepsis was generally not considered to be a cause based on the data reported herein; however, lack of toxic granulation and left shift does not completely exclude sepsis as cause of death as immune suppression may suppress these immune responses. There was evidence of multisystem organ failure in animals that were euthanized prior to the study endpoint. In these animals, no evidence of hemolytic anemia was found.

One of the more intriguing findings was the transient, but significant spike in triglycerides on day 1 post TBI in most ( $n = 17/20$ ), but not all animals. The severe increase in triglycerides was visually evident in blood samples at this time point due to the lactescent plasma, which was confirmed by automatic biochemical analysis of serum samples (e.g. 5.9-fold-increase, on average, in triglycerides above the physiological range). Kaplan-Meier and ROC analysis did not show a correlation between triglyceride levels on day 1 and survival outcomes (Supplemental Figure 1). The lack of correlation; however, does not necessary negate the potential for a biological effect on downstream pathogenesis of radiation-injury in one or more organs. Some moribund animals (28.5%) presented with elevated triglycerides levels at the time of euthanasia prior to the study endpoint of 45-days.

These findings leave open the question of whether hemostatic dysfunction is due to direct endothelial injury, which was not directly assessed in this study due to limitations in availability of antibodies cross-reactive with rabbits, bone marrow failure, or sepsis. Total protein and albumin concentrations were low in all animals at the time of euthanasia, regardless of the time point, which was suggestive of vascular permeability (oncotic pressure), and consistent with petechiae and hemorrhagic lesions observed at necropsy in the majority of moribund animals. In general, the endothelium is often considered an anti-coagulant and loss would lead to coagulation and microthrombi formation rather than diffuse hemorrhage. Cardiac and pulmonary injury may also reduce oxygen delivery causing endothelial injury/hemostatic dysfunction after TBI.

Clotting abnormalities observed in this study, may be suggestive of liver injury and/or vitamin K synthesis. Further, delayed gastric emptying may indicate reduced absorption of a number of fat-soluble vitamins, including Vitamin K, that rely on diet. This is supported by hypoalbuminemia as early as day 1 post-TBI. The study was limited by evaluation of hemostasis and coagulation factor activity at the time of euthanasia due to criteria, or at the scheduled endpoint for study termination. Therefore, natural history studies were designed to better understand the temporal onset, severity, and duration of coagulopathy, and correlation with outcome following TBI (Jackson et al. 2019). The

lingering question unanswered by the current study is the underlying mechanism of mortality associated with multi-organ injury. Knowledge resulting from subsequent natural history studies may provide useful data on phenotypes of radiation injury and response.

In conclusion, the rabbit model of TBI-induced ARS presents with a response similar to that observed in humans (4). Clinical manifestations include pancytopenia and severe hemorrhage progressing to multiorgan failure and mortality or spontaneous recovery with moderate supportive care. ARS in the rabbit may more closely translate to the non-human primate and human than other small animal models, and therefore provides new opportunities for both identification of novel therapeutic targets and medical countermeasure testing to treat the severe hemorrhagic syndrome and improve the likelihood of survival.

## Acknowledgements

The authors gratefully acknowledge our consultants, Dr. Mitchell J. Cohen and Dr. Phillip C. Spinella, whose thoughtful reviews aided in the interpretation of the data generated within this study.

## Disclosure statement

The authors declare no conflicts of interest related to the data generated within this study.

## Funding

This project has been funded in whole with federal funds from the Biomedical Advanced Research and Development Authority, Office of the Assistant Secretary for Preparedness and Response, Department of Health and Human Services under Contract #HHSO1002015000091, Task Order Number HHSO10033001T, entitled “Establishment of a rabbit model of ionizing radiation-induced thrombocytopenia, coagulopathies, and measures of associated vascular and organ injury”.

## Notes on contributors

**Isabel L. Jackson** is an Associate Professor, Radiation Biologist, and Deputy Director of the Division of Translational Radiation Sciences, Department of Radiation Oncology, at the University of Maryland School of Medicine. She is the Director of the division’s Medical Countermeasures program.

**Ganga Gurung** was a Research Associate within the Division of Translational Radiation Sciences, Department of Radiation Oncology, at the University of Maryland School of Medicine. She is now practicing medicine in the United Kingdom.

**Yannick Poirier** is an Assistant Professor and board-certified Clinical Medical Physicist in the Department of Radiation Oncology, Division of Medical Physics and Division of Translational Radiation Sciences at the University of Maryland School of Medicine. He oversees the dosimetry and physics of all radiation biological studies of the Division of Translational Radiation Sciences.

**Mathangi Gopalakrishnan** is an Assistant Research Professor within the Center for Translational Medicine within the University of Maryland School of Pharmacy.

**Eric P. Cohen** is a Professor of Medicine within the University of Medicine School of Medicine.

**Terez Shea-Donohue** was a Professor of Radiation Oncology and member of the Division of Translational Radiation Sciences, Department of Radiation Oncology, University of Medicine School of Medicine. She is now a Program Director, within the Division of Digestive Diseases and Nutrition at the National Institute of Diabetes and Digestive and Kidney Diseases.

**Diana Newman** is a Program Director within the Division of Translational Radiation Sciences, Department of Radiation Oncology, University of Medicine School of Medicine.

**Zeljko Vujaskovic** is a Professor of Radiation Oncology and Director of the Division of Translational Radiation Sciences, Department of Radiation Oncology, University of Medicine School of Medicine.

## References

- Allen JG, Jacobson LO. 1947. Hyperheparinemia: cause of the hemorrhagic syndrome associated with total body exposure to ionizing radiation. *Science*. 105(2728):388–389.
- Cernerud L. 1975. The setting-sun eye phenomenon in infancy. *Dev Med Child Neurol*. 17(4):447–455.
- Copley AL. 1948. The ecchymosis test for capillary hemorrhagic diathesis. *Science*. 107(2773):201–202.
- Cronkite EP. 1950. The hemorrhagic syndrome of acute ionizing radiation illness produced in goats and swine by exposure to the atomic bomb at Bikini, 1946. *Blood*. 5(1):32–45.
- Fliedner TM, Beyrer IF. 2001. Medical management of radiation accidents: manual on the acute radiation syndrome. London: British Institute of Radiology.
- Hall EJ, Giaccia AJ. 2011. Radiobiology for the radiologist. 7th ed. Philadelphia (PA): Lippincott Williams & Wilkins.
- Jackson IL, Gurung G, Ayompe E, Poirier Y, Cohen EP, Cohen MJ, Newman D, Vujaskovic Z. 2019. Characterization of the severe hemorrhagic syndrome in the New Zealand white rabbit model following total body irradiation. *Int J Radiat Biol*. 1–35. DOI: [10.1080/09553002.2020.1820601](https://doi.org/10.1080/09553002.2020.1820601)
- Liebow AA, Warren S, DeCoursey E. 1949. Pathology of atomic bomb casualties. *Am J Pathol*. 25(5):853–1027.
- MacVittie TJ, Farese AM, Bennett A, Gelfond D, Shea-Donohue T, Tudor G, Booth C, McFarland E, Jackson W. 3rd. 2012. The acute gastrointestinal subsyndrome of the acute radiation syndrome: a rhesus macaque model [Research Support, N.I.H., Extramural]. *Health Phys*. 103(4):411–426.
- Mapara M, Thomas BS, Bhat KM. 2012. Rabbit as an animal model for experimental research. *Dent Res J (Isfahan)*. 9(1):111–118.
- Moroni M, Coolbaugh TV, Lombardini E, Mitchell JM, Moccia KD, Shelton LJ, Nagy V, Whitnall MH. 2011. Hematopoietic radiation syndrome in the Gottingen minipig. *Radiat Res*. 176(1):89–101.
- Norris WP, Fritz TE, Rehfeld CE, Poole CM. 1968. The response of the beagle dog to cobalt-60 gamma radiation: determination of the LD50(30) and description of associated changes. *Radiat Res*. 35(3):681–708.
- Norris WP, Poole CM. 1968. The response of beagle dogs to protracted exposure to 60Co gamma-rays at 5-35 R-day. II. Survival and clinical observations. ANL-7535. ANL Rep. 156–157.
- Poirier Y, Prado C, Prado K, Draeger E, Jackson IL, Vujaskovic Z. 2019. Use of CT simulation and 3-D radiation therapy treatment planning system to develop and validate a total-body irradiation technique for the New Zealand White rabbit. *Int J Radiat Biol*. 1–28. DOI:[10.1080/09553002.2019.1665215](https://doi.org/10.1080/09553002.2019.1665215)
- Pryor WH, Jr., Glenn WG, Hardy KA. 1967. The gamma radiation LD 50(30) for the rabbit. *Radiat Res*. 30(3):483–487.

- Shea-Donohue T, Fasano A, Zhao A, Notari L, Yan S, Sun R, Bohl JA, Desai N, Tudor G, Morimoto M, et al. 2016. Mechanisms involved in the development of the chronic gastrointestinal syndrome in non-human primates after total-body irradiation with bone marrow shielding. *Radiat Res.* 185(6):591–603.
- Siller-Matula JM, Plasenzotti R, Spiel A, Quehenberger P, Jilma B. 2008. Interspecies differences in coagulation profile. *Thromb Haemost.* 100(3):397–404.
- UNSCEAR. 2000. Sources, effects, and risks of ionizing radiation. report to the general assembly, Annex J: exposures and effects of the Chernobyl accident. New York (NY): United Nations.
- Warren S. 1946. The pathologic effects of an instantaneous dose of radiation. *Cancer Res.* 6:449–453.
- Warren S, Draeger RH. 1946. The pattern of injuries produced by the atomic bombs at Hiroshima and Nagasaki. *U S Nav Med Bull.* 46: 1349–1353.